Sn(IV)-corroles reversibly bind carboxylates in the axial position

Helle Ø. Bak[a,b], Paolo Cavigli[a], Andrew Bond[c], Theis Brock-Nannestad[b], Michael Pittelkow*[,b] and Elisabetta Iengo*[,a]

[a]*Department of Chemical and Pharmaceutical Sciences, University of Trieste, Via L. Giorgieri 1, 34127 Trieste, Italy*
[b]*Department of Chemistry, University of Copenhagen, Universitetsparken 5, DK-2100, Copenhagen Ø, Denmark*
[c]*Department of Chemistry, University of Cambridge. CB2 1EW, Lensfield Road, United Kingdom*

ABSTRACT: We present the synthesis of Sn(IV)-corrole complexes that bind to carboxylate moieties reversibly, *via* axial ligation. The systems have been predominantly characterized using ^{1}H NMR spectroscopy, X-ray crystallography, and MALDI mass spectrometry. The dynamic nature of the Sn(IV)−O_2CR bond has been studied in solution using 2D-NMR spectroscopy.

KEYWORDS: corrole, Sn(IV), NMR, supramolecular, carboxylate, x-ray, exchange.

INTRODUCTION

The exploration of chemical bonds that are thermodynamically stable, yet kinetically labile, opens interesting possibilities in supramolecular chemistry [1]. One such possibility lies within the expanding field of dynamic combinatorial chemistry, where the liability, and thus resulting reversibility, of certain chemical bonds, allows the exploration of so-called dynamic combinatorial libraries for the identification of novel host-guest systems [2]. It carries significant importance that the reversible chemical reaction in question is orthogonal to (does not interfere with) other chemical processes in the resulting equilibrating system [3].

The widespread use of porphyrins in supramolecular chemistry, with applications in molecular electronics and as mimics of natural systems, has inspired the synthesis and systematic study of the properties of porphyrin and porphyrin-like structures [4]. Both expanded and contracted porphyrinoids have been studied, and many fascinating architectures have been reported [5]. A key contributing researcher in this area is Prof. Sessler [6]. Corroles can be viewed as contracted porphyrins (one *meso*-carbon is missing as compared to porphyrin), as analogs of the cobalt-chelating corrin in vitamin B_{12} (an oxidized corrin), or simply as excellent tri-anionic macrocyclic ligands for metal ions in high oxidation states [7]. Catalysis has been a major driving force in the development of corrole chemistry, due to the ability to host metals in one oxidation state higher than the widely used porphyrins [8]. The chemistry of corroles has experienced a renaissance after the discovery by Goldberg and Gross that triarylcorroles can be formed in appreciable yields in a one-pot procedure from pyrrole and benzaldehyde [9]. To date, much of the attention in corrole research has been concentrated on the synthesis of differently substituted corroles, insertion of different metals, and various applications in biological sciences [10].

Here we present a study of a metallocorrole as a potential building block in supramolecular chemistry, in particular as a mediator of reversible processes. This study

*Correspondence to: Prof. Dr. E. Iengo, Department of Chemical and Pharmaceutical Sciences, University of Trieste, Via L. Giorgieri 1, 34127 Trieste, Italy. E-mail: eiengo@units.it, Prof. Dr. M. Pittelkow, Department of Chemistry, University of Copenhagen, Universitetsparken 5, DK-2100, Copenhagen Ø, Denmark. E-mail: pittel@chem.ku.dk

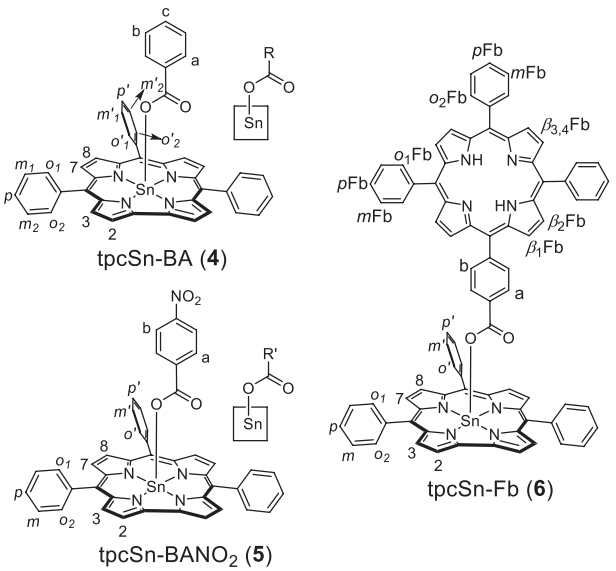

Fig. 1. Drawings of the Sn(IV)(carboxylate)-corroles derivatives reported in this work, with relevant ^{1}H NMR labeling schemes.

is the first description of Sn(IV)(carboxylate)-corroles (**4-6**, Fig. 1), and we use triphenyl-corrole **tpcSn-Cl** (**1**, Scheme 1) as starting platform to establish the synthetic chemistry, the binding properties of carboxylates and conditions for carboxylate exchange reactions. Specifically, we sought to identify a new metal-ligand system to be used together with both Al(III)(carboxylate)-porphyrins [11] and Sn(IV)(carboxylate)$_2$-porphyrins [12] for the construction of dynamic combinatorial libraries based on the exchange of the metal-carboxylate bond as a reversible reaction. A complicating factor in the use of the porphyrin-based systems is the fact that the metal ions have a tendency to coordinate two ligands, axially bound on either side of the metallated porphyrin. In metalated corroles the metal ion is often situated slightly outside the plane of the corrole ligand, this turns out also to be the case for the Sn(IV)-corrole systems [13]. Furthermore, a distinct difference between porphyrins and corroles, is that corroles are trianionic ligands, while porphyrins are dianionic ligands. For these reasons, it was expected that the tin only coordinates axial ligands on one face of the corrole thus making the system more well-defined. The Sn(IV)(carboxylate)-corroles incorporate a metal ion that enables us to study the system by simple NMR spectroscopy in order to achieve structural and dynamics information. To the best of our knowledge, this is the first reported study on Sn(IV)(carboxylate)-corroles. Moreover, these systems absorb visible light strongly and possess redox properties, which potentially would give access to dynamic multi-chromophore systems for light-harvesting and electron-transfer applications [14].

RESULTS AND DISCUSSION

Triphenylcorroles derived from benzaldehyde and pyrrole were used in this study, and they were prepared using the known protocol described previously by condensing the appropriate benzaldehyde directly with pyrrole in propionic acid (Scheme 1) [9]. While free-base corroles

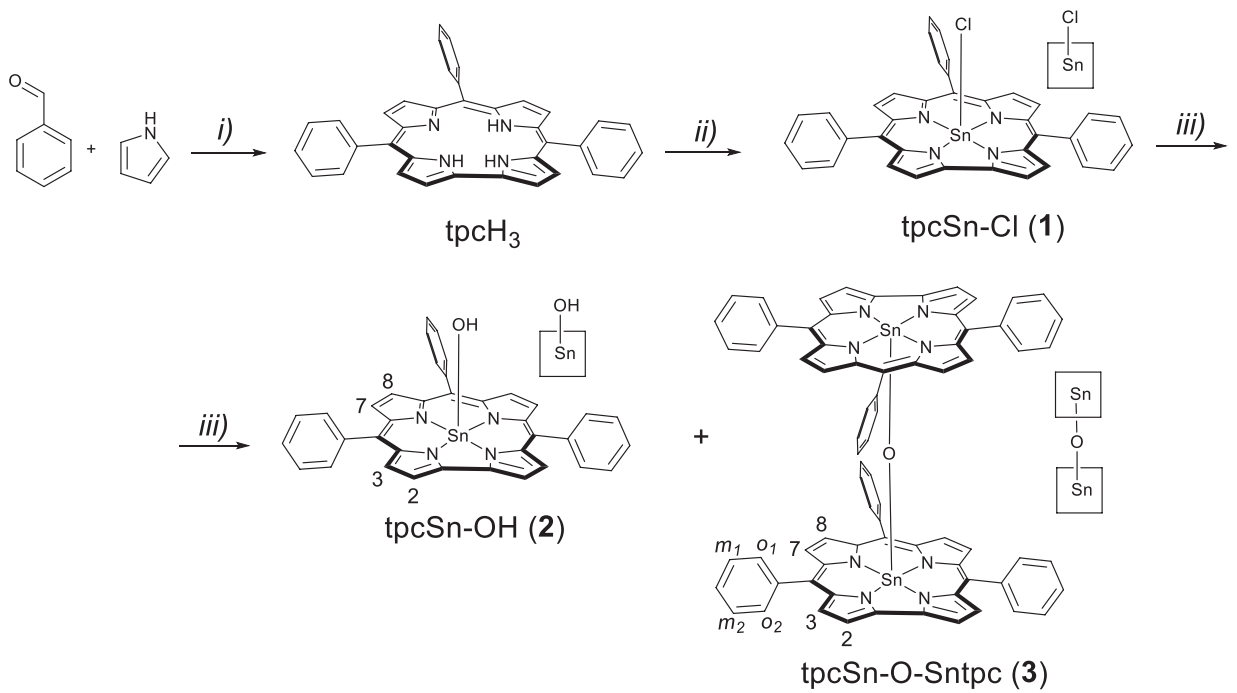

Scheme 1. Synthetic sequence used to prepare Sn(IV)-corroles, and ^{1}H NMR relevant labeling scheme; i) propionic acid, 9%, ii) $SnCl_2$, DMF, 24%, iii) pyridine, then Al_2O_3, 50% (combined yield of 2 and 3).

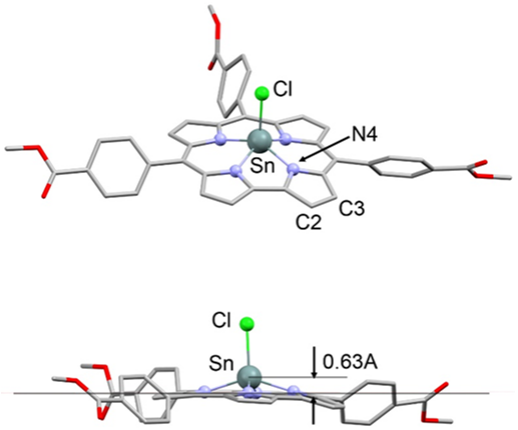

Fig. 2. Two views of the X-ray structure of **tpcCOOMeSn-Cl**. H atoms and disorder of the methylbenzoate groups are omitted. Bottom: side view showing the displacement of tin from the mean plane containing the four N atoms. Selected bond distances (Å) and angles (°): Sn–N 2.035(2)–2.041(2), Sn–Cl 2.3236(7); N–Sn–N (*cis*) 76.44(9)–90.09(10), N–Sn –N (*trans*) 141.78(10)–144.26(10), N–Sn–Cl 105.16(8) – 109.74 (6).

often have limited stability at ambient conditions in solutions, the corrole gained significant chemical stability after the insertion of the Sn(IV) ion. Storing the various derivatives of Sn(IV)-corroles at room temperature for months at ambient conditions presented no problem. Sn(IV) insertion proceeds smoothly by treatment of corrole (**1**) with $SnCl_2$ in warm dimethylformamide (DMF), and the structure was confirmed by ^{1}H-NMR analysis and MALDI-TOF mass spectrometry (see Experimental Section and Supplemental Materials).

A single crystal of a Sn(IV)Cl-triphenylcorrole derivative (**tpcCOOMeSn-Cl**) was obtained by us in a previously published work [15] from a corrole-bearing methyl ester substituents on the *para* position of phenyl groups [16]. The X-ray crystallographic analysis confirmed that the tin cation is five coordinates and located considerably outside the mean plane of the corrole (Fig. 2). In fact, the Sn(IV) center exhibits a square-pyramidal coordination geometry (Addison τ_5 parameter = 0.04) [17], and is displaced by 0.63 Å from the mean plane defined by the four N atoms of the macrocycle in line with distances reported for other Sn–Cl corrole complexes [18]. Further images and details on this structure, as well as comparison with other Sn(IV)X-corrole (X = Cl, CH_3, $(CH_2)_2COOCH_3$, C_6H_5) solid-state structures and data refinement descriptions are given in the Supplemental Material.

Hydrolysis of **tpcSn-Cl** (**1**) proceeds at room temperature in THF/H_2O by treatment with basic Al_2O_3 to yield the **tpcSn-OH** (**2**) derivative together with its μ-*oxo* homodimer **tpcSn-O-Sntpc** (**3**) (see Scheme 1). The two products **2** and **3** are found to be equilibrating by water exchange (hydrolysis), as confirmed by ^{1}H NMR ($CDCl_3$) analysis. The dynamic equilibrium between **2** and **3** causes the room temperature ^{1}H-NMR (wet $CDCl_3$, Fig. 3) of **2** and **3** in $CDCl_3$ to be composed of two sets of resonances of different intensity, with the minor set appearing as quite broad; the water peak is shifted downfield as a result of the participation in the equilibrium (the H_2O/HOD broad resonance is found at δ = 4.65 ppm, in contrast to the typical δ = 1.56 ppm shift for the same species in $CDCl_3$, see also Fig. S6). Upon cooling of the sample all the signals sharpen to give an almost perfect first-order spectrum below −40 °C, with the appearance of two clear sets of β-protons (unambiguous assignments of most of the resonances was done by a combination of HH COSY and ROESY experiments at −50 °C (see Supplemental Materials and below). The signals with major intensity were attributed to the **tpcSn-O-Sntpc** μ-oxo corrole species **3**, according to their more upfield δ values that result from the mutual shielding of the tin-corrole moieties, while the minor set was attributed to **2**. In the HH-ROESY spectrum exchange peaks

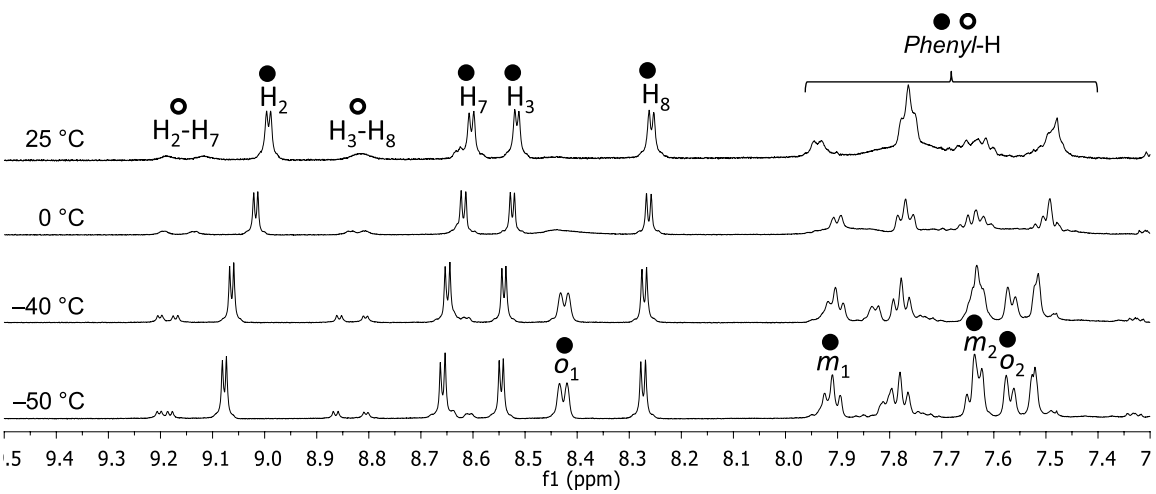

Fig. 3. VT ^{1}H NMR experiment (500 MHz, $CDCl_3$), aromatic region, of the **tpcSn-OH** (**2**) and **tpcSn-O-Sntpc** (**3**) product mixture deriving from the hydrolysis of **tpcSn-Cl** (**1**); empty and full circles identify **2** and **3**, respectively, see Scheme 1 for the relevant proton labeling.

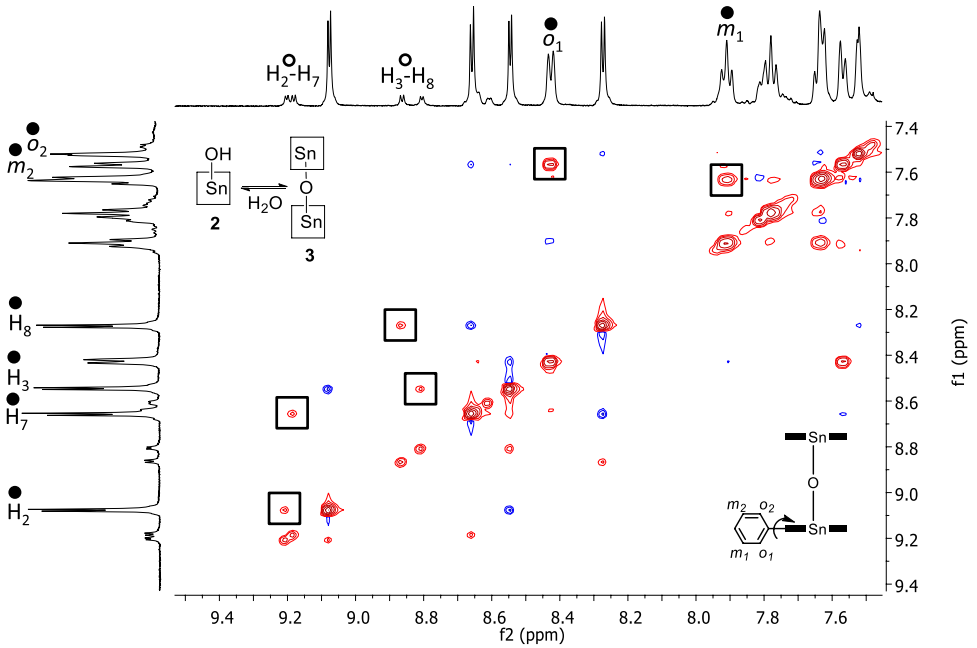

Fig. 4. HH-ROESY spectrum (500 MHz, $CDCl_3$, −50 °C) of the **2** + **3** equilibrating mixture. Strong exchange peaks are observed between the two equilibrating species and between the signals of inner and the outer o_2 and o_1 *ortho* and m_2 and m_1 *meta* protons, pairwise interconverting by 180° rotation of the phenyl rings, of **3**.

were observed between the pyrrole protons in **2** and **3**, confirming that the two species exchange dynamically (Fig. 4). It must be noted that, upon lowering the temperature, in concomitance with the decrease of the exchange rate between **2** and **3** also the slow rotation of the aryl substituents around the C_{meso}–C_{ring} is observed. This fact is evidenced by the sharpening, resolution, and splitting of some of the phenyl proton signals of **3** at −50 °C, and by the related exchange-correlation found in the ROESY spectrum at the same temperature (Fig. 4). Finally, an experiment with the addition of D_2O and saturation of chloroform was conducted. The spectrum registered at 25 °C in dry chloroform presents sharp resonances and closely resembles that registered at −50 °C in wet chloroform, aside from the broad and unresolved signals of some of the proton of the phenyl residues (see Fig. S4 and S5 in the SI); the **Sn-OH/Sn-O-Sn** ratio, by relative integration of the *beta* signals, was estimated to be 1/8 under these conditions. The addition of D_2O resulted in a general broadening of the *beta* resonances and in an increase of the minor signals at 8.85 and 9.15 ppm (see Fig. S5); confirming both that the latter belongs to **Sn-OH/tpcSn-OD** and the presence of an equilibrium process between **2** and **3**. Attempts to precisely determine the coalescence temperatures (and derive exchange rates values) for the two dynamic processes (*i.e.* exchange between **2** and **3** and phenyl groups rotation) were not performed at this stage, but surely the T_C for both is above 25 °C in $CDCl_3$.

In the MALDI-TOF spectrum of **2** + **3** equilibrating mixture, the main peak is related to the dominant **tpcSn-O-Sntpc** species (Fig. S7 in the SI). A very minor peak was corresponding to the mass of $tpcSn^+$ was also found, while tpcSn-OH is only observed in trace amounts. Further examples of metallocorroles as μ-oxo-complexes have been reported in the literature including Nardis *et al.* who reported μ-oxo trisphenylcorroles with Fe and Ge as the metal [19], and Gross' Fe(IV)-corrole μ-oxo-complexes [20]. While to our surprise, despite the ease of the hydrolysis reaction (also associated with the strong oxophylicity of the Sn(IV) cation), only a brief mention of a corroleSn-OH species is reported in the literature [10a].

Sn(IV)(carboxylate)-corroles

The displacement of the axially bound Cl-ligand in corrole-Sn(IV)-Cl (**1**) proceeds very slowly (days) when treated with benzoic acid (see Fig. S14). However, after removal of the chloride, the Sn(IV)-corroles mixture of **2** and **3** reacts with benzoic acid (BA) rapidly (within few minutes, *i.e.* time for the NMR sample preparation and registering) by simple addition of the acid to a chloroform solution of the mixture to give **tpcSn-BA** (**4**) with almost complete conversion when a 1:1 ratio of acid to Sn-corrole units is reached, as evaluated from signal relative integration (Fig. 5). The ^1H NMR spectrum confirmed the coordination of the benzoate by the upfield shifts found for the benzoate proton resonances (Δδ for the Ha, Hb and Hc of −1.53 ppm, −0.96 ppm and −0.65 ppm, respectively, Fig. 5 and Fig. S9), due to the shielding effect of the corrole. The Δδ values observed are smaller compared to the typical ones found for benzoates axially bound to Sn(IV)-porphyrins [12], indicating either a larger distance of the benzoate moiety from

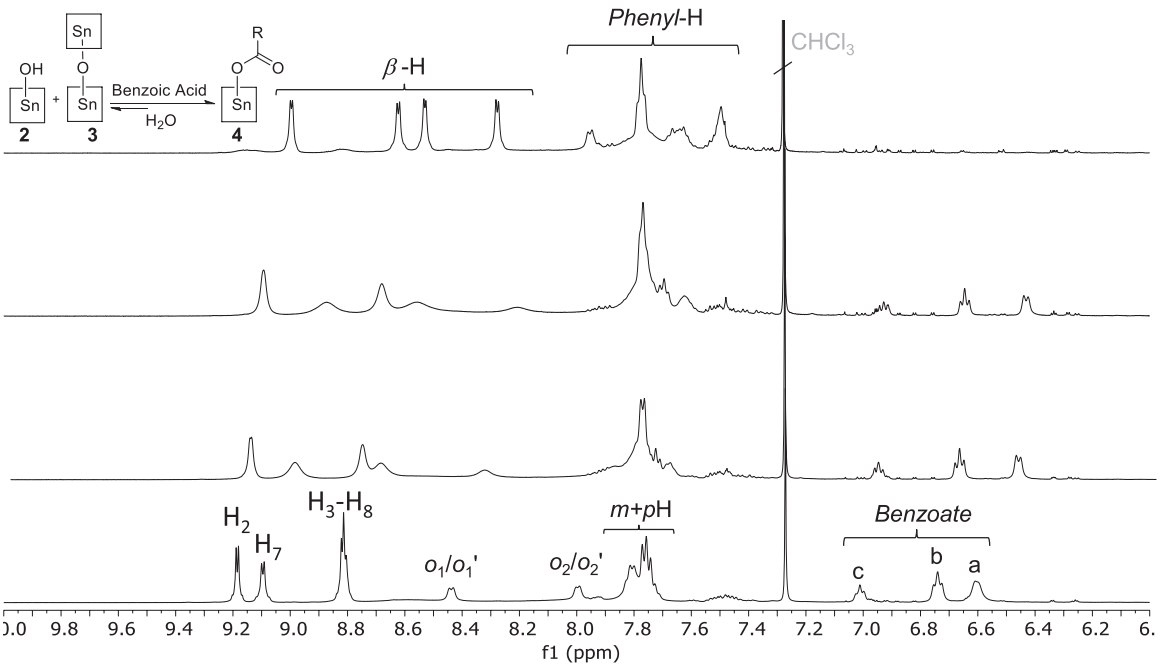

Fig. 5 ^{1}H NMR (500 MHz, $CDCl_3$, 25 °C) spectra of the **2** + **3** equilibrating mixture, top, and of gradual conversion of this mixture to **tpcSn-BA** (**4**) by progressive addition of benzoic acid - complete conversion is observed when a 1:1 ratio between Benzoic Acid and Sn-corrole unit is reached, bottom. The two middle spectra correspond to qualitatively assessed sub-stoichiometric additions of BA to the **2** + **3** mixture; see Scheme 1 and Fig. 1 for relevant proton labeling.

the aromatic corrole ring current or a minor aromaticity character of the corrole ring, with the former being more likely as the tin atom is found to be located outside the plane of the corrole due to the smaller size of macrocycle's metal binding cavity (see above), as compared to a porphyrin (see Fig. S9 for comparative ^{1}H NMR spectra). The resonances of the corrole moiety broaden along with the progressive addition of the benzoic acid, indicating the presence of an equilibrium shifted towards the formation of **tpcSn-BA** (**4**) and sharpen when the 1:1 ratio is reached (Fig. 5, bottom). In this latter situation the presence of the benzoate group in the axial position of the metal is evident from the resolution and large splitting of the ortho phenyl protons residing either above or below the macrocycle plane (see also SI for assignments), while all of the other phenyl proton signals present extended overlap. The large splitting found for the ortho protons unambiguously indicates that in chloroform solution the rotation of the Sn-corrole phenyl groups is slow already at roomT. Increasing the ratio above 1:1 results in a broadening and progressive downfield shift of the axial ligand proton signals toward the δ-value of pure benzoic acid (Fig. S10 in SI).

A mixture containing **tpcSn-OH+tpcSn-O-Sntpc** and **tpcSn-BA** in an approximate weighted 1:1 ratio (*i.e.* regarding the **2** + **3** samples as solely composed by **3**) has been prepared and investigated by VT ^{1}H NMR to elucidate the kinetics of the equilibrium between **2** + **3** and **4** (Fig.6). The spectrum at room temperature is very broad and difficult to interpret, while upon lowering the temperature down to −50 °C the low field signal pattern clearly indicates the presence of equilibrium between free (**2** + **3**) and bound (**4**) Sn-corroles (Fig. 6). Correct correlations and exchange between the β-protons and few of the resolved phenyl protons are found in the HH COSY and HH ROESY spectra, see also Fig. S10 and S11. Still, both the lack of peaks coalescence and clean resolution upon increasing or lowering the temperature hampers the ability to gather quantitative information on the kinetic and thermodynamic parameters of the equilibrium, at this stage. Further proof of the exchange process evidenced above was inferred by a similar experiment done on the same mixture with a lower ratio of the **tpcSn-BA** component (see Fig. S13).

p-Nitro benzoic acid reacts with the **tpcSnOH/tpcSn-O-Sntpc** mixture in a similar manner to benzoic acid, leading to the formation of **tpcSnBA-NO$_2$** (**5**); a comparison of the ^{1}H NMR spectrum of **tpcSn-BA** (**4**) and **tpcSn-BANO$_2$** (**5**) is shown in Fig. 7 (Δδ for Ha and Hb of −1.66 ppm and −0.82 ppm, respectively).

In Sn-porphyrins changes in acid strength of the axial carboxylate ligands affect the δ-values, and competitive ligand exchange is observed. As has become clear from our studies, this trend is not clearly observed in the case of the Sn-corroles, and benzoic acids with different acidities appear to bind equally well.

Based on the coordination sphere of the Sn(IV) when bound to the corrole and a chloride ligand (Fig 2) and the fact that 1:1 complexes are formed with carboxylates, we are confident that the Sn-atom in the tpcSn-BA complexes has the Sn atom situated slightly outside the

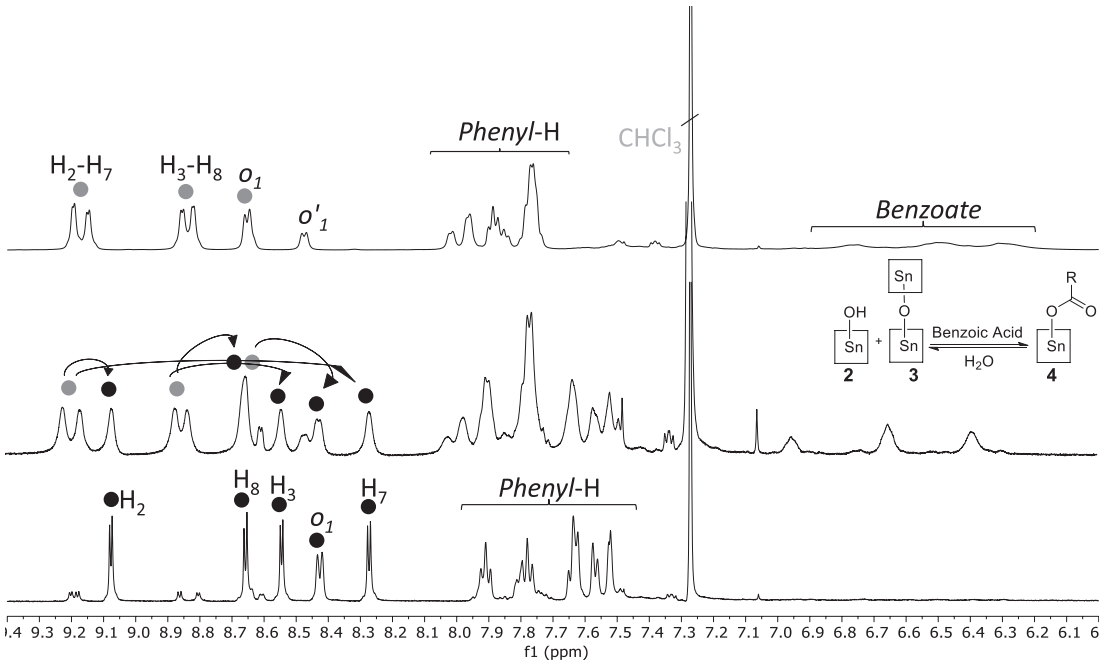

Fig. 6. [1]H NMR spectra (500 MHz, $CDCl_3$, −50 °C) of: top) **tpcSn-BA**; middle) a 1/1 mixture of **tpcSn-OH+tpcSn-O-Sntpc** (black circles) and **tpcSn-BA** (grey circles); arrows identify the exchange peaks between the relevant and resolved proton resonances found in the HH ROESY spectrum (see also Fig. S12); bottom) **tpcSn-OH + tpcSn-O-Sntpc**.

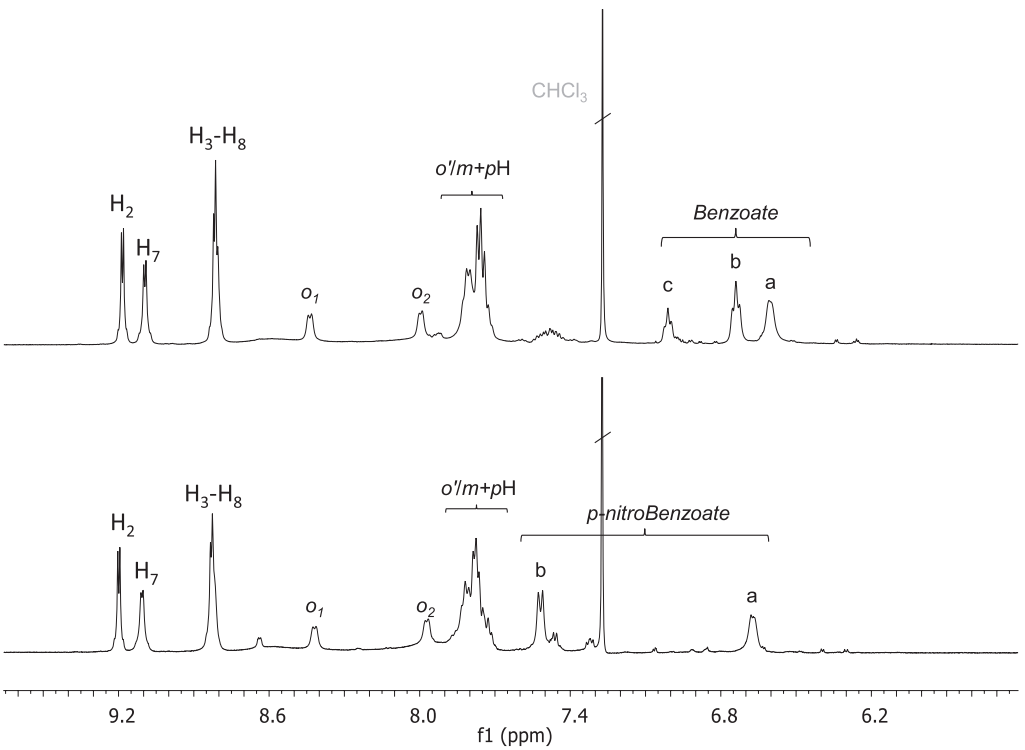

Fig. 7. [1]H NMR (500 MHz, $CDCl_3$, 25 °C) spectra of **tpcSn-BA** (**4**), bottom, and **tpcSn-BANO$_2$** (**5**), top; see Fig. 1 for relevant proton labeling.

plane of the corrole. For this reason, we did not expect the Sn-atom to have any additional axial ligands bound (as Sn-porphyrins do) and we confirmed this by NMR spectroscopy and did not observe any changes in the [1]H-NMR spectra upon the addition of nitrogen-based ligands such as picoline.

The ability of tpcSn-OH to quickly and reversibly bind benzoic acid moieties with the formation of a relatively

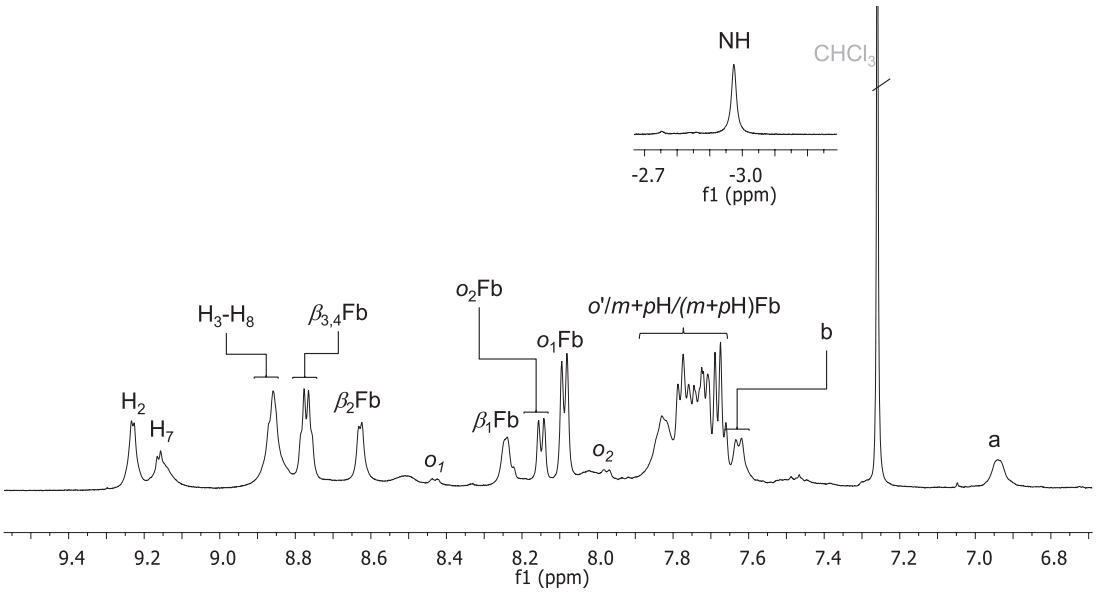

Fig. 8. ^{1}H NMR (500 MHz, $CDCl_3$, selected regions, 25 °C) spectrum of **tpcSn-Fb** (**6**), see Fig. 1 for relevant proton labeling scheme and Fig. S16 for 2D assignments.

stable carboxylate axial bond was exploited to survey the possibility of constructing more intriguing conjugates. In particular, the **tpcSn-OH/tpcSn-O-Sntpc** mixture was subjected, at room temperature in chloroform solution, to one equivalent of 5-(4-Carboxyphenyl)-10,15,20-trisphenyl porphyrin (**Fb**), and the resulting mixture, analyzed by ^{1}H-NMR, is in agreement with the formation of the one to one di-chromophoric conjugate **tpcSn-Fb** (**6**) (Fig. 1 and Fig. 8 and Fig. S16). As expected, the main consequence of the axial coordination to the Sn-corrole is a remarked upfield shift of the proton resonances of the axially bound **Fb** porphyrin compared to the parent free system, with an extent that decreases as the proton distance from the Sn(IV)-corrole plane increases (*e.g.*, $\Delta\delta$ = −1.57, Ha; −0,74, Hb; −0.60, β_1Fb; and −0.22, β_2Fb). As noted above for tcpSn-BA, this effect is less marked than the analogue containing a Sn(IV)-porphyrin connected axially to two Fb units [21]. As far as the overall spectral features are concerned (in terms of chemical shift values, resolution and diffused broadness) these are quite similar to the ones discussed above for **tpcnSn-BA**, and coherent with the presence of a fast equilibrium between the Sn-corrole and Fb building units, shifted towards the assembled **tpcSn-Fb** conjugate. It should be noted that the MALDI-TOF analysis of these conjugates reveals only the corrole-Sn^+ ions, and that assignment of their structure is for the moment based on NMR studies.

CONCLUSIONS

To conclude, we have described the first example of a metallocorrole that may be employed as a functional building block in supramolecular chemistry, also in complement to other similar yet distinct units such as metalloporphyrins, for the dynamic assembling of larger multicomponent, possibly multichromophoric, structures. In particular by simple hydrolysis of Sn(IV) Cl-triphenylcorrole, a mixture of hydroxy and μ-oxo Sn(IV)-corroles is obtained, that readily reacts with carboxylic acids, with the formation of a single reversible tin-carboxylate axial bond. Selectivity towards oxygen-containing ligands and five-coordination geometry of tin was observed by NMR spectroscopy. A single crystal X-ray structure of a Sn(IV)Cl-corrole gives further structural insights into the nature of the system, indeed the Sn-atom is found to be located outside the plane of the corrole, well explaining the selectivity towards 5-coordination. The fact that the Sn(IV)-atom is sitting outside the plane of the π-conjugated corrole is evident also in the ^{1}H-NMR spectra of coordinated carboxylates that are found to be less affected by proximity to the π-conjugated system, as compared to metalloporphyrin analogues. The reversibility of the newly formed tin-carboxylate bond was demonstrated by NMR analysis. Future prospects include the preparation of Sn(IV)-corroles equipped with different carboxylate moieties to combine the dynamic Sn(IV)-corroles with other metal complexes in order to create complex dynamic combinatorial libraries.

EXPERIMENTAL

General

All chemicals, including were purchased from Sigma-Aldrich and used as received. Solvents were of reagent grade. Triphenylcorrole tpcH3 and (4-Carboxyphenyl)-10,15,20-trisphenyl porphyrin were prepared according to literature procedures [16, 21] 1D

and 2D NMR spectra were recorded at room temperature – unless stated otherwise – on a Varian 500 spectrometer (^{1}H: 500 MHz, ^{13}C{^{1}H}: 125.7 MHz) ; ^{1}H chemical shifts were referenced to the peak of residual non-deuterated solvent (δ = 7.26 for $CDCl_3$); selected carbon resonances were assigned through the HSQC spectra. Reactions were followed using MALDI-TOF and TLC. MALDI-TOF was performed on a Bruker Autoflex Speed mass spectrometer with dithranol as matrix and analyzed with DataAnalysis v. 4.0 SP5. Merck DCAlufolien SiO_2 60 F254 0.2 mm thick precoated TLC plates were used for TLC. The plates were analyzed/visualized under UV-light at 254 and 366 nm. Purifications: Dry column vacuum chromatography, using silica gel 15–40 μm from ROCC S.A./N.V, and technical or HPLC grade solvents were used for purifications. Melting points were measured using a Stuart™ melting point apparatus SMP3, and are uncorrected. MALDI-HRMS and ESI-HRMS were performed on a Bruker SolariX XR 7T ESI/MALDI FTMS spectrometer with dithranol as a matrix. External calibration of the spectrometer was conducted with sodium trifluoroacetate cluster ions. X-ray crystallographic data were collected using a Nonius KappaCCD diffractometer with Mo Kα radiation (λ= 0.7107 Å). The temperature was held at 150(2) K using an Oxford Cryosystems N_2 cryostat. Data integration and reduction were undertaken with HKL Denzo/Scalepack [22] and a multi-scan correction was applied using SORTAV [23]. The structure was solved using SHELXT [24] and refined using SHELXL [25]. The structure contains solvent molecules ($CHCl_3$ and/or hexane) which were difficult to refine by conventional methods. The solvent content was therefore treated using a continuous solvent area model with the SQUEEZE algorithm [26]. Further details are given in the Supplemental Materials.

Acknowledgments

M. Pittelkow appreciates the support from the Danish Council for Independent Research (DFF 4181-00206 and 9040-00265) and from the University of Copenhagen. E. Iengo gratefully acknowledges the financial support from the University of Trieste (FRA2022).

REFERENCES

1. Steed JW and Atwood JL. Supramolecular Chemistry (3rd Edn), Wiley, 2022.
2. Corbett PT, Leclaire J, Vial L, West KR, Wietor JL, Sanders JKM and Otto S. *Chem. Rev.* 2006; **106**: 3652–3711.
3. Rasmussen B, Sørensen A, Beeren SR and Pittelkow M. In: *Organic Synthesis and Molecular Engineering*, John Wiley & Sons, **2013**, 393–436.
4. (a) Marchini M, Luisa A, Bergamini G, Armaroli N, Ventura B, Baroncini M, Demitri N, Iengo E and Ceroni P. *Chem. Eur. J.* 2021; **27**: 16250–16259. (b) Natali M, Amati A, Demitri N and Iengo E. *Chem. Commun.* 2018; **54**: 6148–6152. (c) Bols SB and Anderson HL. *Acc. Chem. Res.* 2018; **51**: 2083–2092.
5. Wang Y, Ke XS, Lee S, Kang S, Lynch VM, Kim D and Sessler JL. *J. Am. Chem. Soc.* 2022; 144: 9212–9216.
6. Arambula JF and Sessler JL. *Chem* 2020; **6**: 1634–1651.
7. Natale CD, Gros CP and Paolesse R. *Chem. Soc. Rev.* 2022; **51**: 1277–1335.
8. Sinha W, Mahammed A, Fridman N and Gross Z. *ACS Catal.* 2020; **10**: 3764–3772.
9. (a) Gross Z, Galili N and Saltsman I. *Angew. Chem., Int. Ed.* 1999; **38**: 1427–1429. (b) Gross Z, Galili N, Simkhovich L, Saltsman I, Botoshansky M, Blaser D, Boese R and Goldberg I. *Org. Lett.* 1999; **1**: 599–602.
10. (a) Paolesse R. In Porphyrin Handbook; Kadish, KM, Smith, KM and Guilard, R, Eds.; Academic Press: San Diego, CA, 2000; Vol. 2, pp. 201–232. (b) Orlowski R, Gryko D and Gryko DT. *Chem. Rev.* 2017; **117**: 3102–3137. (c) Nardis S, Mandoj F, Stefanelli M and Paolesse R. *Coord. Chem. Rev.* 2019; **388**: 360–405.
11. (a) Iengo E, Pantoş GD, Sanders JKM Orlandi M, Chiorboli C, Fracasso S and Scandola F. *Chem. Sci.* 2011, **2**: 676–685. (b) Metselaar GA, Sanders JKM and Mendoza J. *Dalton Trans.* 2008; 588–590. (c) Davidson GJE, Tong LH, Raithby PR and Sanders JKM. *Chem. Commun.* 2006; 3087–3089.
12. (a) Hawley JC, Bampos N, Sanders JKM and Abraham RJ *Chem. Commun*. 1998; 661–662. (b) Arnold DP and Blok J. *Coord. Chem. Rev.* 2004; **248**: 299–319. (c) Shetti VS, Pareek Y and Ravikanth M. *Coord. Chem. Rev.* 2012; **23–24**: 2816–2842.
13. (a) Wang Z, Yao Z, Lyu Z, Xiong Q, Wang B and Fu X. *Chem. Sci.* 2018; **9**: 4999–5007. (b) Sinha W, Kumar M, Garia A, Pyrohit CS, Som T and Kar S. *Dalton Trans.* 2014; **4**: 12564–12573.
14. Berna BB, Platzer B, Wolf M, Lavarda G, Nardis S, Galloni P, Torres T, Guldi DM and Paolesse R. *Chem. Eur. J.* 2020; **26**; 13451–13461.
15. Bak HØ. PhD thesis, University of Copenhagen, **2013**.
16. Pittelkow M, Brock-Nannestad T, Bendix J and Christensen JB. *Inorg. Chem.* **2011; 50**; 5867–5869.
17. Addison AW, Rao NT, Reedijk J, van Rijn J and Verschoor GC. *J. Chem. Soc. Dalton Trans.* 1984: 1349–1356.

18. a) Sinha W, Kumar M, Garai A, Purohit CS, Som T and Kar S. *Dalton Trans.* 2014; **43**: 12564–12573. (b) Wagnert L, Berg A, Stavitski E, Berthold T, Kothe G, Goldberg I, Mahammed A, Simkhovich L, Gross Z and Levanon H. *Appl. Magn. Reson.* 2006; **30**: 591–604.
19. (a) Nardis S, Mandoj F, Paolesse R, Fronczek FR, Smith KM, Prodi L, Montalti M and Battistini G. *Eur. J. Inorg. Chem.* 2007; 2345. (b) Sorokin AB *Coord. Chem. Rev.* 2019; **389**: 141–160.
20. (a) Simkhovich L, Mahammed A, Goldberg I, Gross Z, *Chem Eur. J.* 2001, **7**, 1041–1055. (b) Aviv-Harel I and Gross Z., *Coord. Chem. Rev.*, 2011, **255**, 717–736.
21. Amati A, Cavigli P, Demitri N, Natali M, Indelli, MT and Iengo E. *Inorg. Chem.* 2019; **58**: 4399–4411.
22. Otwinowski Z and Minor W. *Methods in Enzymology*, 1997; **276**: 307–326.
23. Blessing RH. *Acta Crystallogr. Sect. A,* 1995; **51**: 33–38.
24. Sheldrick GM. *Acta Crystallogr. Sect. A,* 2015; **71**: 3–8.
25. Sheldrick GM. *Acta Crystallogr. Sect. C*, 2015; **71**: 3–8.
26. Spek AL. *Acta Crystallogr. Sect. C*, 2015; C**71**: 9–18.